Alexander, S., Eastoe, J., Lord, A. M., Guittard, F., & Barron, A. R. (2016). Branched Hydrocarbon Low Surface Energy Materials for Superhydrophobic Nanoparticle Derived Surfaces. *ACS Applied Materials and Interfaces*, *8*(1), 660-666. https://doi.org/10.1021/acsami.5b09784

Article

Branched Hydrocarbon Low Surface Energy Materials (LSEMs) for Superhydrophobic Nanoparticle Derived Surfaces

Shirin Alexander, Julian Eastoe, Alex M. Lord, Frederic Guittard, and Andrew R Barron

ACS Appl. Mater. Interfaces, **Just Accepted Manuscript** • DOI: 10.1021/acsami.5b09784 • Publication Date (Web): 07 Dec 2015

Branched Hydrocarbon Low Surface Energy Materials (LSEMs) for Superhydrophobic Nanoparticle Derived Surfaces

Shirin Alexander,[†] Julian Eastoe,[‡] Alex M. Lord,[§] Frédéric Guittard,[ξ] and Andrew R. Barron[†,¶,ß]

[†] Energy Safety Research Institute (ESRI), Swansea University Bay Campus, Fabian Way, Swansea, SA1 8EN, UK

[‡] School of Chemistry, University of Bristol, Bristol, BS8 1TS, UK

[§] Centre for Nanohealth (CNH), College of Engineering, Swansea University, Singleton Park, SA2 8PP, Wales, UK.

[ξ] University of Nice Sophia Antipolis, CNRS, LPMC, Group surfaces & interfaces, Parc Valrose, 06100 Nice, France

[¶] Department of Chemistry, Rice University, Houston, TX 77005, USA.

[ß] Department of Materials Science and Nanoengineering, Rice University, Houston, Texas 77005, USA.

ABSTRACT. We present a new class of superhydrophobic surfaces created from low-cost and easily synthesized aluminum oxide nanoparticles functionalized carboxylic acids having highly branched hydrocarbon (HC) chains. These branched chains are new low surface energy materials (LSEMs) which can replace environmentally hazardous and expensive fluorocarbons (FCs). Regardless of coating method and curing temperature, the resulting textured surfaces develop water contact angles (θ) of ~155° and root-mean-square roughnesses (R_q) ≈ 85 nm, being comparable with equivalent FC functionalized surfaces (θ = 157º and R_q = 100 nm). The functionalized nanoparticles may be coated onto a variety of substrates to generate different superhydrophobic materials.

KEYWORDS: superhydrophobic hydrocarbon surfaces, alumina nanoparticles, low surface energy materials, fluorinated acids, hyperbranched carboxylic acids

INTRODUCTION

The most remarkable property of low surface energy materials (LSEMs) is their superhydrophobic performance, as exemplified by a water contact angle (θ) larger than 150°.[1] Although originally found naturally, for example with Lotus leaves and some insect wings, the potential applications (including, repellent surfaces, water-proof textiles, papers, and fibers[2-5]) have encouraged synthetic mimicry. For Lotus leaves the high $\theta \sim 170°$ is a result of cutin and lipid coverings as well as a hierarchical micro and nano double surface structures.[6,7] The latter feature is considered crucial for achieving superhydrophobicity, as chemical factors alone can only develop contact angles less than 120°.[8] Thus, superhydrophobic surfaces have generally been obtained by adsorption or attachment of coatings to substrates by combining micro/nanomaterials (to introduce surface roughness) with self-assembled monolayers of low surface energy materials (LSEMs) (to introduce appropriate surface chemistry).[9-11] Superhydrophobicity can be achieved from either textured surfaces with inherent hydrophobicity

(carbon nanostructures[12]), or more effectively through addition of a suitable chemical functionality to textured surfaces: for example, grafting fluorinated polymers onto raspberry-like (RB) nanoparticles (NPs),[13] addition of fluorinated silanes to graphene oxide particles,[6] applying polydimethylsiloxane (PDMS) in conjunction with functionalized titania, Fe_3O_4, Ni, CoO, and silica NPs,[7,8,14] oxide surfaces with coated perfluorononane and vinyl terminated poly(dimethylsiloxane),[15] PTFE-coated carbon nanotubes,[16] and also n-dodecanethiol coatings for silver aggregates.[17] In addition diamond-like carbon (DLC) coatings have also shown superhydrophobic behavior based on the nature of the plasma used in the pre-treatment.[18,19]

Where chemical modification is required, to date, the majority of representative superhydrophobic surfaces have been obtained by introducing fluorocarbon (FC) functionalities.[10,20-22] Unfortunately, this has important environmental consequences because of the persistence, bioaccumulation, and toxicity of long chained FCs.[22-24] It is obviously desirable to prepare hierarchical micro/nano structures in parallel with simple non-hazardous chemical functionalization, but using non-fluorinated surface treatments.

It was shown previously that the use of zwitter ionic carboxylic acids enables formation of superhydrophilic nanoparticle surfaces which induce collapse of aspirated water droplets onto a surface,[25] as well as oil/water separation membranes.[18,26] The structure of these nanoparticle coatings was found to be textured at the micro scale, but created from nano aggregates.[27] Clearly, the same approach in combination with typical FC functionality would be expected to perform as a superhydrophobic coating, as has been reported.[10] However, it is of greater interest to know whether any alternative surface functionalities may be used with lower environmental impacts. In this regard, it has been reported that single chain hydrocarbon (HC) surfactants, synthesized from commercially available highly branched "hedgehog" alcohols, can be used to generate

effective LSEMs.[28] These new low surface energy surfactants (with improved water solubility compared to the long chain, linear HC analogue) can reduce the surface tension of water to an all-time low value for single chain HC surfactants of 24 mN m^{-1}.[28-30] Herein are demonstrated effective and simple formulations to obtain environmentally safe and economic superhydrophobic surfaces, using relatively short, highly branched hydrocarbon chains, and commercially available "hedgehog" carboxylic acids to functionalize alumina nanoparticles. Although this methodology can be applied to a variety of NPs, alumina NPs were chosen as a model core system as these NPs are among the most commercially important nanoparticles with a wide range of applications. A summary of this approach is shown in Scheme 1.

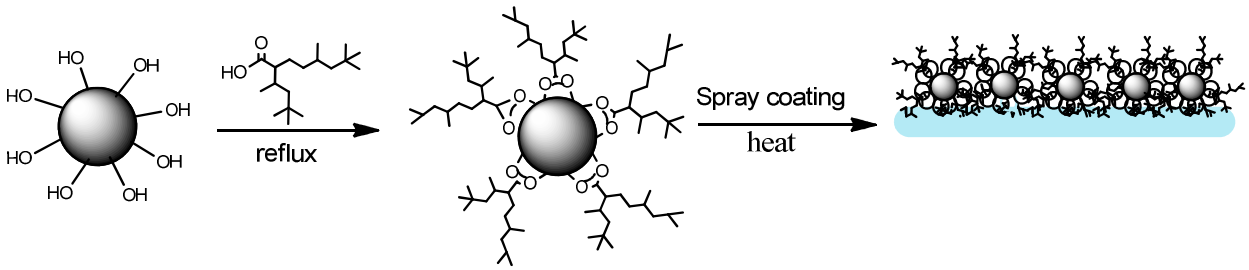

Scheme 1. Schematic representation of the approaches used to obtain superhydrophobic surfaces.

EXPERIMENTAL SECTION

Materials and Reagents. Alumina NPs (Aeroxide-Alu), perfluorotetradecanoic acid, 9H-hexadecafluorononanoic acid, stearic acid, 2-propanol, and ethanol were purchased from Sigma Aldrich and used as received. Isostearyl acids were obtained from Nissan Chemical Industries and used without further purification. Distilled water (Millipore, 15 MΩ cm) was used throughout the experimental process.

Surface and Nanoparticle Characterization. Thermogravimetric analysis (TGA) experiments were conducted on a TA Instrument SDT Q600. The samples were run in an open

alumina crucible under continuous air flow. The heating profile was equilibrated at 50 ºC and then ramped at 20 ºC.min^{-1}. Scanning electron microscopy (SEM) was performed with a Hitachi field emission S-4800 microscope. Fourier transform infrared (FTIR) measurements were performed with a Thermoscientific i510 recording spectra in the 400-4000 cm^{-1} region with 16 scans. Contact angle measurements were obtained by the sessile drop method (resulting static contact angle data) using a drop shape analysis program, DSA1, (Krüss, FM40 easydrop instrument) under ambient conditions using DI water. Each stated contact angle is the average of three measurements from various positions on the surface. Atomic force microscopy (AFM) and non-contact cantilevers (RTESP, Bruker) were used for surface imaging. Images for each sample were obtained using intermittent contact mode, at a scan rate of 0.5-1 Hz and an image resolution of 512 x 512 pixels. Images were obtained with a scan size of 10 x 10 μm. The captured images were analyzed using JPK offline-processing software to determine the surface roughness from the AFM scans. The mean roughness measurements determined the average (R_a), root-mean-square (R_q), and peak-to-valley roughness (R_t) for each sample type. Nanoparticle size distribution was obtained by using a Zetasizer Nano (Nano ZS), Malvern instrument. The solutions were prepared by weighing 0.05 wt % of the nanoparticles in 2-propanol and dispersing using a sonic bath for 30 minutes. The samples were then left on a roller mixer for 24 h to reach equilibrium, before measurements. The presented data are the average value of three measurements.

Synthesis of Carboxylate Functionalized Nanoparticles. In a modification to the reported procedures in the literature,[25,31] the alumina NPs were refluxed overnight in toluene (100 mL) with the appropriate carboxylic acid: isostearyl acids, fluorinated carboxylic acids and stearic acid. The functionalized particles were then centrifuged for 30 minutes, and then re-dispersed in

2-propanol (2 x 30 mL) and ethanol (1 x 30 mL) and then centrifuged again in order to remove unreacted carboxylic acid. Finally particles were oven dried at 80 ºC overnight.

Spray Coating of Nanoparticle Films. Nanoparticle dispersions in 2-propanol (2 wt%**)** were sprayed onto substrates, including glass slides, cardboard or paper. The slides were heated at 80 ºC during the spray coating. The spray coating was performed until a film was optically visible. The glass coated surfaces were therefore slightly bluish and completely transparent. Some slides were dried at either 25 °C or 40 ºC to show the effect of drying temperature on the water contact angle (see Table 1). In the case of glass coated surfaces, the films can get scratched and removed if get contact by a sharp material, however, the cardboard or paper coated particles are long-lasting and durable.

Spin Coating of Nanoparticle Films. Nanoparticle dispersions in 2-propanol (2 wt%**)** were spin coated onto glass slides under a nitrogen atmosphere, using a WS-650-23 Laurell spin coater. The dispersions (3 x 200 µL) were placed on a clean slide and spun at 8000 rpm and accelerated at 300 rpm followed by more of the dispersion (2 x 200 µL) added to the spinning surfaces. The coated substrates were then dried at 80 ºC on a hot plate for 20 minutes.

RESULTS AND DISCUSSION

Aluminum oxide wafers/nanoparticles can be covalently functionalized by different bifunctional acids (as molecular anchors), and self-assembled mono- or multi-layers may be formed based on the nature of the carboxylic acid.[32] The alumina NPs used in this study have an average particle size of d = 13 nm and specific surface area of 100 ±15 $m^2.g^{-1}$. In the formulation carboxylic acids were chosen based on previous work with branched chain systems:[28] iso-stearic acid (**I**) and iso-stearic acid-N (**II**) with branching factor of 7.1 and 6.6 and effective linear chain length of 13.6

n_c and 15 n_c, respectively.[28] These new systems were compared with two fluorinated surfaces, obtained using standard commercially available FCs, perfluorotetradecanoic acid (**III**) and 9H-hexadecafluorononanoic acid (**IV**).

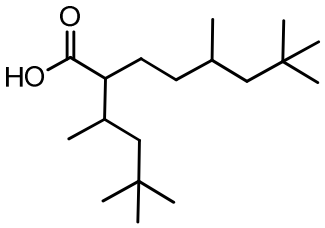

(I)

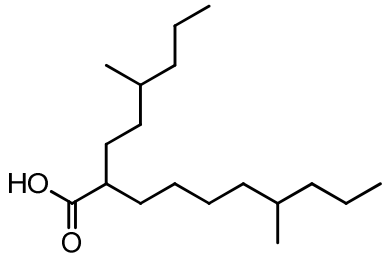

(II)

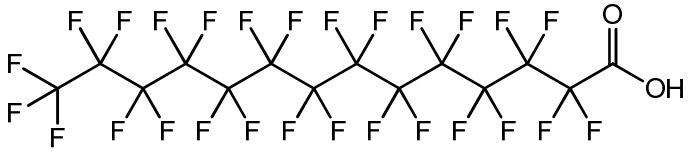

(III)

(IV)

Functionalization of aluminum oxide nanoparticles. The alumina NPs (Aeroxide-Alu C, Sigma Aldrich) were refluxed overnight in toluene (100 mL) in the presence of the appropriate carboxylic acid.[27,32] The extent of functionalization was determined by TGA (Figure 1; for comparison TGA traces of native carboxylic acids is provided in Figure S1). The as-received alumina NPs show no significant mass loss <800 °C (Figure 1a); however, after functionalization with carboxylic acids, changes began at approximately 300 ºC with rapid weight loss occurring in the range 350-400 ºC (Figure 1b-e). It should be noted that the TGA trace of perfluorotetradecanoic acid functionalized NPs (Figure 1e) shows an additional mass loss (3.5%)

at around 200 ºC. This is due to excess acid that was difficult to remove without repeated purification; however, appropriate corrections were made for calculating the grafting density.

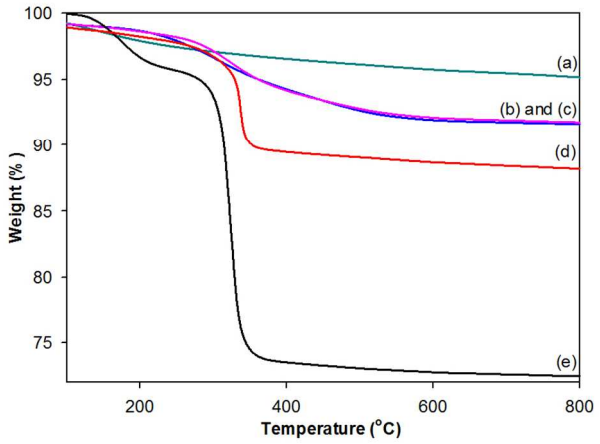

Figure 1. TGA of (a) unfunctionalized alumina NPs and alumina NPs functionalized with (b) iso-stearic acid-N, (c) iso-stearic acid, (d) 9H-hexadecafluorononanoic acid, and (e) perfluorotetradecanoic acid.

The surface coverage of the acids was calculated for each carboxylic acid functionalized NP system (Supporting Information), and presented in Table 1. For normal, less bulky, linear chain carboxylic acids[33,34] a grafting density of 9.4 per nm^2 would be consistent with surface saturation. It can be seen from the grafting densities shown in Table 1, that as may be expected, branched and bulky surfactants suffer steric hindrance at the interface, which leads to lower surface grafting densities compared to linear chain analogues.

Table 1. Contact angle measurements for unmodified nanoparticles and various modified nanoparticle surfaces.

Carboxylic acid functionalized NP	Effective chain length n_c	Grafting density (nm^{-2})	θ(°) spray coating[a]	θ(°) spin coating[a]
-	-	-	22±2	-
iso-stearic-N acid ($C_{17}H_{35}CO_2H$)	15	2.1	153±3	152±2
iso-stearic acid ($C_{17}H_{35}CO_2H$)	13.5	2.0	154±2	153±2
			153±2 (40 ºC)	
			153±2 (25 ºC)	
perfluorotetradecanoic acid ($C_{13}F_{27}CO_2H$)	14	2.7	157±3	-
9H-hexadecafluorononanoic acid ($C_8F_{16}HCO_2H$)	7	1.9	137±3	-

[a] All samples were dried at 80 ºC unless otherwise stated.

FTIR-ATR spectra of carboxylic functionalized NPs (Figure 2) confirm covalent attachment of the carboxylate moieties. In each case, after reaction with the NP surface the C=O stretching band of the carboxylic acid (ca. 1700 cm^{-1})[35] is replaced by bands at 1400 cm^{-1} and 1600 cm^{-1} due to the symmetric and asymmetric stretches of carbonyls in bidentate modes (Figure 2).[33] Concomitant with these changes is the decrease in the broad band at 3464 cm^{-1} due to the presence of hydrogen bonded OH groups on the nanoparticle surfaces.[35] The peaks at 2963 cm^{-1} and 2929 cm^{-1} are due to the aliphatic C–H stretches of HC acids (Figure 2b and c), whereas for the FC systems (Figure 2d and e), the presence of very strong peaks at around 1148 cm^{-1} to 1400 cm^{-1} are due to $C–F_2$ and $C–F_3$ vibrations.[10] The peak at 1756 cm^{-1} for the perfluorotetradecanoic acid derivative (Figure 2e), assigned as C=O stretching, is also observed in the free acid (Figure S2),[36] suggesting the existence of unreacted acids, in agreement with the TGA data.

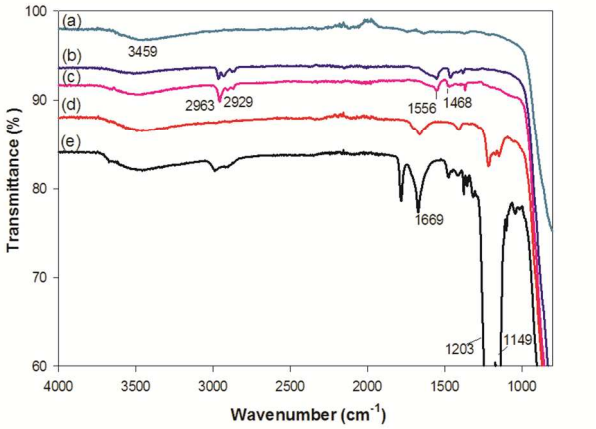

Figure 2. FTIR-ATR spectra of (a) unfunctionalized alumina NPs, and NPs functionalized with (b) iso-stearic acid-N, (c) iso-stearic acid, (d) 9H-hexadecafluorononanoic acid, and (e) perfluorotetradecanoic acid.

The nanoparticles were also analyzed by dynamic light scattering (DLS) in 2-propanol to investigate a hydrodynamic diameter (d_h), which initially showed that 0.05 wt% unfunctionalized alumina particles have a d_h = 250 ±5 nm with a polydispersity index (PDI) of 0.25 which indicates agglomeration of the particles. In the case of the functionalized particles, all samples yielded d_h of around 160-170 nm with PDI = 0.15-0.20. The 0.05 wt % dispersed solutions used for DLS (shown in Figure S3a) were stable for several weeks. Photographic images of 0.5 wt % functionalized nanoparticles dispersed in 2-propanol after 30 minutes and after 3 days are shown in Figure S3b-c of the supporting information. The images show that apart from 9H-hexadecafluorononanoic particles that showed signs of precipitation after 1 day (due to the lower number of grafts, hence higher particle-particle interactions), the particles were stable for at least 3 days.

Surface nanostructures. It was previously shown that carboxylate functionalized alumina NPs may be rendered immobile through heating at a moderate temperature, without significantly

effecting the surface properties.[25] Thus, in order to produce superhydrophobic surfaces, nanoparticles were dispersed in 2-propanol (2 wt%) and then spray coated onto microscope slides at 80 ºC. Alternatively, the dispersions were spin-coated and subsequently heated to 80 °C for 20 mins. Films may be deposited on a wide range of substrates; however to demonstrate proof-of-principle, films were deposited on glass slides. The coated surfaces were then analyzed by contact angle measurements, SEM and AFM.

Static equilibrium contact angle (θ) measurements for the various carboxylic acid functionalized surfaces are summarized in Table 1, and photographic images of droplets are shown as inserts in Figure 3. Pieces of cardboard and medical wipe were also spray coated with iso-stearic acid functionalized particles, and the morphology (Figure S6 and S7) and wetting behavior of the cardboard is shown in Supporting Information.

Hydrophobicity of a surface varies widely with the nature of functionalized groups, and surface free energy decreases in the sequence $CF_3 < CF_2H < CF_2 < CH_3 < CH_2$.[28,37,38] Based on this trend it is expected that the highest contact angle would occur for FC surfaces. However, spray coated films of branched HC materials (iso-stearic and iso-stearic-N acids) also revealed superhydrophobic properties with contact angle of DI water >153º, comparable with the FC functionalized surfaces (θ = 157º). These remarkably high contact angles occur, despite surface densities of only ca. 2 nm^{-2} highly branched acid molecules on the NPs (in comparison with ca. 3 nm^{-2} for long FC acids adsorbed at NP surfaces, Table 1). It is proposed that the high contact angle is as a direct consequence of increasing the CH_3:CH_2 ratio per acid chain compared to normal linear HC chains: this increased CH_3:CH_2 is a result of branching, hence exposing more –CH_3 groups with the “hedgehog” tail structures. This is in line with previous work, showing that highly branched surfactants can lower the surface tension of water to limiting values

corresponding to pure alkanes.[28,39] The contact angle of 9H-hexadecafluorononanoic acid coated particles is lower (θ = 137º ±3). This is expected because the chain termini are H-CF_2- groups rather than CF_3-: the substitution of F for H results in a dipole moment of ~ 1.5 D at this "sweet spot" in the molecule, hence increasing the hydrophilicity of the surfaces compared to fully fluorinated chain analogues.[40,41] In addition, it known that as contact angle increases with increasing fluorinated/hydrocarbon tail length.[21,22]

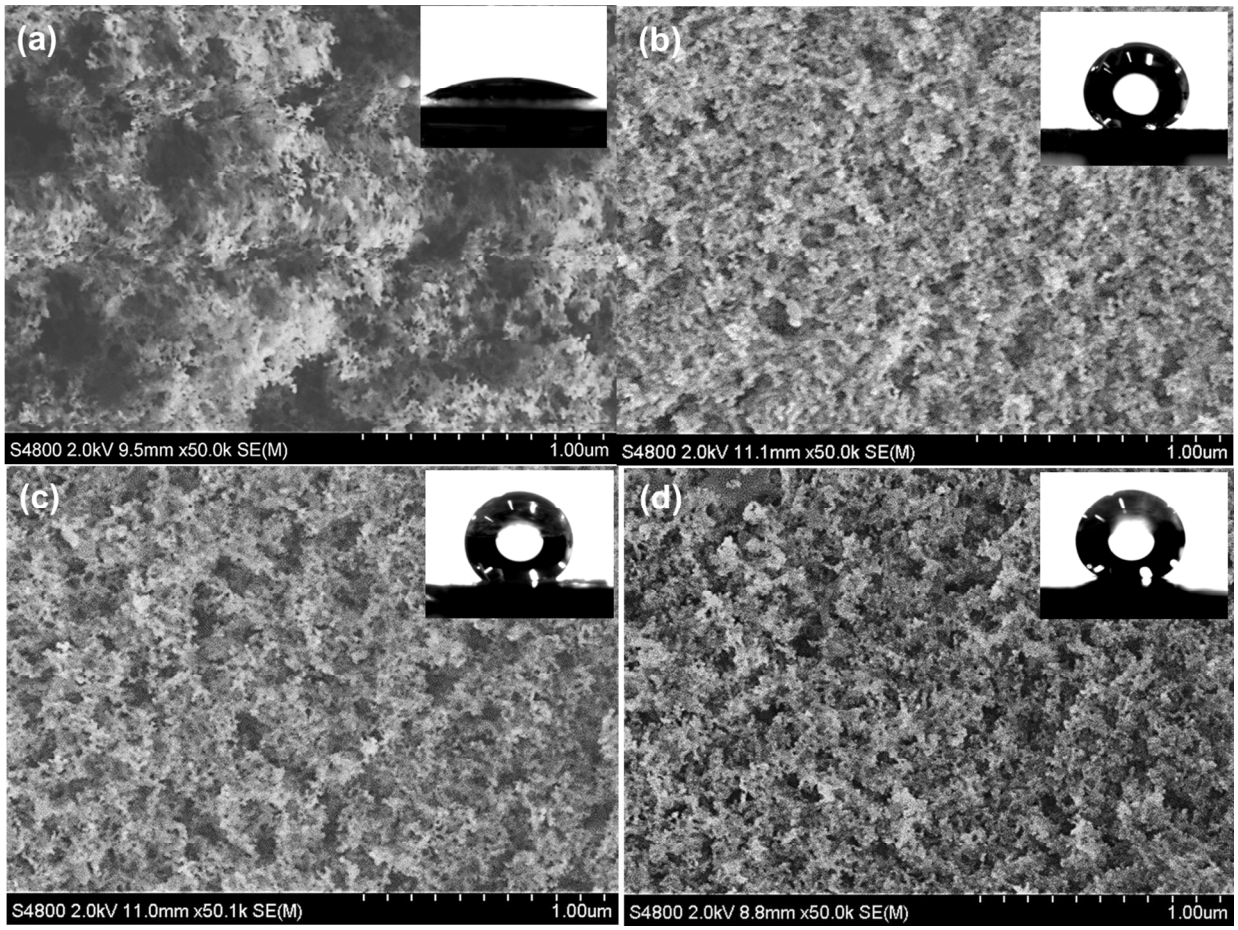

Figure 3. SEM images of films spray coated onto a microscope slide of (a) unfunctionalized alumina nanoparticles, as compared to alumina nanoparticles functionalized with (b) iso-stearic-N, (c) iso-stearic, and (d) perfluorotetradecanoic acids. Inset are photographs of water droplets on the appropriate surface.

SEM images of the modified NP films (Figures 3b-d), show a distinctive change in the surface morphology when compared to the unmodified NPs deposited in a similar manner (Figure 3a). The particles modified with iso-stearic-N, iso-stearic, and perfluorotetradecanoic acids have quite similar surface morphologies, which consists of NPs aggregated into a complex porous structure. It is known that super-hydrophobic coatings formed of textured structures entrap a thin air layer at the surface, and the images in Figure 3 are consistent with air entrainment. The functionalized particles appear to be packed much more efficiently than unmodified particles, generating more highly porous surfaces. This differences in packing indicate a distinct change in the particle surface properties after functionalization, as shown by the contact angle measurements described above.

The two branched HC functionalized particles were used as model compounds for spin coating onto substrates at room temperature. The results (Table 1) indicate that superhydrophobic surfaces can be obtained by using these LSEMs regardless of the coating method. The effect of changing drying temperature of the nanoparticle films was also tested for the iso-stearic acid functionalized alumina NPs. As can be seen, there is no significant difference in water contact angle at two different temperatures (40 ºC and 25 ºC). This indicates that heating to 80 °C does not cause loss of surface coating, and also that solvent evaporation rate does not significantly affect the morphology, roughness, and assembly of the grafted acids on the surface. SEM images of the surfaces dried at 40 ºC and 25 ºC are shown in Figure S4 (Supporting Information).

The film roughnesses were measured using AFM and the results are shown in Table 2 and Figure 4. The roughnesses with functionalized NPs are considerably larger than for unfunctionalized NPs. However, it should be noted that in the case of unfunctionalized alumina NPs, obtaining images with a scan size of 10 x 10 μm was not possible, as the particles would

move when contacted by the probe when imaged in intermittent contact mode. The best possible image was obtained with a scan size of 2.5 x 2.5 μm, as is shown in Figure 4a. The RMS roughness (R_q) values for films formed from iso-stearic acid functionalize NPs is about 100 nm compared to the unfunctionalized surfaces with $R_q \sim 60$ nm. Increases in roughness can account for some of the observed increase in contact angle based on the Wenzel and Cassie theory;[42-43] however, the similarity of the HC to FC functionality suggests that the film texture is not the sole reason.

Table 2. Roughness parameters for unfunctionalized, and various functionalized, particles (spray coated unless otherwise stated) obtained by AFM measurements.

Surface functionalization	Averaged roughness R_a (nm)	RMS roughness R_q (nm)	Peak to valley roughness R_t (nm)
Unfunctionalized alumina NPs	47	60	499
iso-stearic acid-N acid (spray coating)	65	84	781
iso-stearic acid-N acid (spin coating)	60	75	550
iso-stearic acid	85	111	1200
perfluorotetradecanoic acid	124	155	1002
9H-hexadecafluorononanoic acid	62	78	634

Surfaces of spin coated iso-stearic acid-N particles were also analyzed by SEM and AFM, and images are shown in Figure S5 of the supporting information. The surface morphologies are very similar to the spray coated analogues; however, the surfaces are slightly smoother (Table 2) resulting in a slight decrease in hydrophobicity as is shown in Table 1. This is due most likely to the use of the mechanical coating technique rather than spray-coating, as the latter process may

be used for a wider range of substrates. For example, films can be readily deposited on glass, fabric, paper and cardboard, and in each case the superhydrophobic surfaces show similar properties. A video demonstration of the wetting is provided in the Supporting Information.

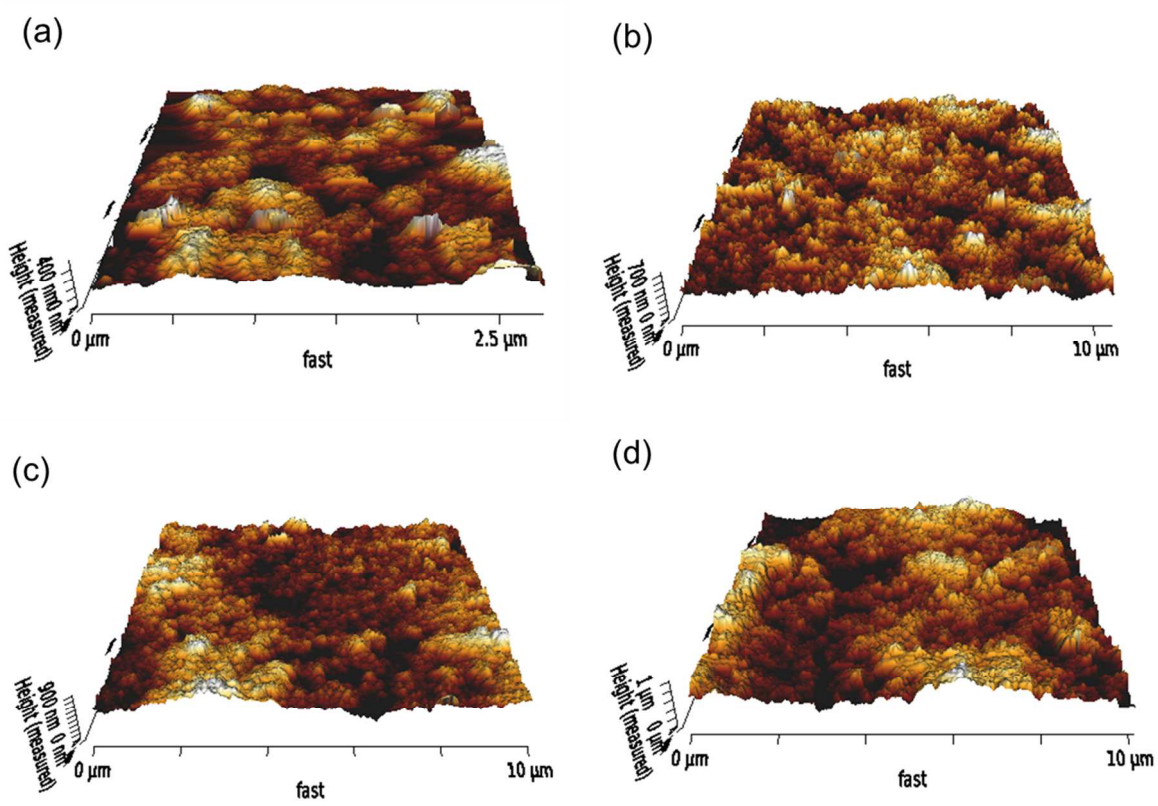

Figure 4. AFM topography images of (a) unfunctionalized alumina NPs, and alumina NPs functionalized with (b) iso-stearic-N acid, (c) iso-stearic acid, and (d) perfluorotetradecanoic acid.

CONCLUSIONS

Simple, low cost and hydrocarbon based superhydrophobic surfaces may be successfully prepared using alumina NPs chemically functionalized with highly branched "hedgehog" low surface energy carboxylic acids. Whereas prior work has shown that superhydrophobic surfaces may be prepared using fluorocarbon surfactants and polymers,[10,13,6,20,22,44] this work

demonstrates for the first time, that superhydrophobic surfaces (contact angle ~155º) can be obtained using relatively short chained highly branched hydrocarbon chains (n_c =13 and 15). This superhydrophobicity is achieved by combining the surface roughness of nanoparticle-derived films and low surface energy properties of the highly branched alkyl chains coating the NPs. It is known that branched HC chain architectures promote efficient packing at the surface of aqueous solutions, allowing densely packed disordered films promoting low surface tensions (energies)[28]. Hence, it can be assumed that similar high surface density structures are also present at the surface of NPs. These nontoxic and cheap hydrocarbon-based LSEMs have much potential for new coating applications on a variety of substrates, and as a replacement for costly, hazardous fluorocarbons. A further advantage of this current method over such processes as diamond-like carbon coating is the simplicity of application.[18,19]

ASSOCIATED CONTENT

Supporting Information

The Supporting Information is available free of charge on the http://pubs.acs.org. TGA of the carboxylic acids used for surface functionalization of the alumina nanoparticles. SEM and AFM images of nanoparticles coated on the glass, cardboard, and paper substrates. Video showing the wetting behavior of a piece of cardboard coated with iso-stearic functionalized alumina particles.

AUTHOR INFORMATION

Corresponding Author

*E-mail: a.r.barron@swansea.ac.uk (A.R.B)

Author Contributions

The manuscript was written through contributions of all authors. All authors have given approval to the final version of the manuscript.

Notes

The authors declare no competing financial interest.

ACKNOWLEDGMENTS

Financial support was provided by the Welsh Government Sêr Cymru Programme and the Robert A. Welch Foundation (C-0002). J.E. acknowledges the EPSRC for funding through EPSRC EP/K020676/1 under the G8 Research Councils Initiative on Multilateral Research Funding - G8-2012.

REFERENCES

(1) Wang, S.; Jiang, L. Definition of Superhydrophobic States. *Adv. Mater.* **2007**, *19*, 3423–3424.

(2) Callow, M. E.; Fletcher, R. L. The Influence of Low Surface Energy Materials on Bioadhesion: a Review. *Int. Biodeterior. Biodegrad.* **1994**, *34*, 333-348.

(3) Tsibouklis, J.; Nevell, T. G. Ultra-Low Surface Energy Polymers: The Molecular Design Requirements. *Adv. Mater.* **2003**, *15*, 647-650.

(4) Schmidt, D. L.; Coburn, C. E.; DeKoven, B. M.; Potter, G. E.; Meyers, G. F.; Fischer, D. A. Water-based Non-Stick Hydrophobic Coatings. *Nature* **1994**, *368*, 39-41.

(5) Matsumoto, Y.; Yoshida, K.; Ishida, M. A Novel Deposition Technique for Fluorocarbon Films and Its Applications for Bulk- And Surface-Micromachined Devices. *Sens. Actuators, A* **1998**, *66*, 308-314.

(6) Lin, Y.; Ehlert, G. J.; Bukowsky, C.; Sodano, H. A. Superhydrophobic Functionalized Graphene Aerogels. *ACS Appl. Mater. Interfaces* **2011**, *3*, 2200-2203.

(7) Crick, C. R.; Bear, J. C.; Southern, P.; Parkin, I. P. A General Method for the Incorporation of Nanoparticles into Superhydrophobic Films by Aerosol Assisted Chemical Vapour Deposition. *J. Mater. Chem. A* **2013**, *1*, 4336-4344.

(8) Crick, C. R.; Bear, J. C.; Kafizas, A.; Parkin, I. P. Superhydrophobic Photocatalytic Surfaces through Direct Incorporation of Titania Nanoparticles into a Polymer Matrix by Aerosol Assisted Chemical Vapor Deposition. *Adv. Mater.* **2012**, *24*, 3505-3508.

(9) Celia, E.; Darmanin, T.; Taffin de Givenchy, E.; Amigoni, S.; Guittard, F. Recent Advances in Designing Superhydrophobic Surfaces. *J. Colloid Interface Sci.* **2013**, *402*, 1-18.

(10) Portilla, L.; Halik, M. Smoothly Tunable Surface Properties of Aluminum Oxide Core–Shell Nanoparticles by a Mixed-Ligand Approach. *ACS Appl. Mater. Interfaces* **2014**, *6*, 5977-5982.

(11) Ma, M.; Hill, R. M. Superhydrophobic Surfaces. *Curr. Opin. Colloid Interface Sci.* **2006**, *11*, 193-202.

(12) Hong, Y. C.; Uhm, H. S. Superhydrophobicity of a Material Made From Multiwalled Carbon Nanotubes. *Appl. Phys. Lett*. **2006**, 88, 244101.

(13) Jiang, W.; Grozea, C. M.; Shi, Z.; Liu, G. Fluorinated Raspberry-like Polymer Particles for Superamphiphobic Coatings. *ACS Appl. Mater. Interfaces* **2014**, *6*, 2629-2638.

(14) Facio DS.; Mosquera MJ. Simple Strategy for Producing Superhydrophobic Nanocomposite Coatings In Situ on a Building Substrate. *ACS Appl. Mater. Interfaces* **2013**; *5*, 7517-7526.

(15) Guo, Z.; Zhou, F.; Hao, J.; Liu, W. Stable Biomimetic Super-Hydrophobic Engineering Materials. *J. Am. Chem. Soc.* **2005**, *127*, 15670-15671.

(16) Lau, K. K. S.; Bico, J.; Teo, K. B. K.; Chhowalla, M.; Amaratunga, G. A. J.; Milne, W. I.; McKinley, G. H.; Gleason, K. K. Superhydrophobic Carbon Nanotube Forests. *Nano Lett.* **2003**, *3*, 1701-1705.

(17) Shi, F.; Niu, J.; Liu, J.; Liu, F.; Wang, Z.; Feng, X. Q.; Zhang, X. Towards Understanding Why a Superhydrophobic Coating Is Needed by Water Striders. *Adv. Mater.* **2007**, *19*, 2257-2261.

(18) Cortese B.; Caschera D.; Federici F.; Ingo GM.; Gigli G. Superhydrophobic Fabrics for Oil-Water Separation Through a Diamond Like Carbon (DLC) Coating. *J. Mater. Chem. A* **2014**; *2*, 6781-6789.

(19) Caschera D.; Mezzi A.; Cerri L.; de Caro T.; Riccucci C.; Ingo G.; Padeletti G.; Biasiucci M.; Gigli G.; Cortese B. Effects of Plasma Treatments for Improving Extreme Wettability Behavior of Cotton Fabrics. *Cellulose* **2014**; *21*, 741-756.

(20) Darmanin, T.; Guittard, F.; Amigoni, S.; Tafin de Givenchy, E.; Noblin, X.; Kofman, R.; Celestini, F. Superoleophobic Behavior of Fluorinated Conductive Polymer Films Combining Electropolymerization and Lithography. *Soft Matter* **2011**, *7*, 1053-1057.

(21) Darmanin, T.; Guittard, F. Fluorophobic Effect for Building up the Surface Morphology of Electrodeposited Substituted Conductive Polymers. *Langmuir* **2009**, *25*, 5463-5466.

(22) Darmanin, T.; Guittard, F. Superoleophobic Surfaces with Short Fluorinated Chains? *Soft Matter* **2013**, *9*, 5982-5990.

(23) Begley, T. H.; White, K.; Honigfort, P.; Twaroski, M. L.; Neches, R.; Walker, R. A. Perfluorochemicals: Potential Sources of and Migration from Food Packaging. *Food Addit. Contam.* **2005**, *22*, 1023-1031.

(24) Prevedouros, K.; Cousins, I. T.; Buck, R. C.; Korzeniowski, S. H. Sources, Fate and Transport of Perfluorocarboxylates. *Environ. Sci. Technol.* **2005**, *40*, 32-44.

(25) Maguire-Boyle, S. J.; Liga, M. V.; Li, Q. Barron, A. R. Alumoxane/Ferroxane Nanoparticles for the Removal of Viral Pathogens: The Importance of Surface Functionality to Nanoparticle Activity. *Nanoscale* **2012**, *4*, 5627-5632.

(26) Maguire-Boyle, S. J.; Barron, A. R. A New Functionalization Strategy for Oil/Water Separation Membranes. *J. Membr. Sci.* **2011**, *382*, 107-115.

(27) Callender, R. L.; Harlan, C. J.; Shapiro, N. M.; Jones, C. D.; Callahan, D. L.; Wiesner, M. R.; Cook, R.; Barron, A. R. Aqueous Synthesis of Water-Soluble Alumoxanes: Environmentally Benign Precursors to Alumina and Aluminum-based Ceramics. *Chem. Mater*. **1997**, *9*, 2418-2433.

(28) Alexander, S.; Smith, G. N.; James, C.; Rogers, S. E.; Guittard, F.; Sagisaka, M.; Eastoe, J. Low Surface Energy Surfactants with Branched Hydrocarbon Architectures. *Langmuir* **2014**, *30*, 3413-3421.

(29) Eastoe, J.; Nave, S.; Downer, A.; Paul, A.; Rankin, A.; Tribe, K.; Penfold, J. Adsorption of Ionic Surfactants at the Air−Solution Interface. *Langmuir* **2000**, *16*, 4511-4518.

(30) Mohamed, A.; Sagisaka, M.; Guittard, F.; Cummings, S.; Paul, A.; Rogers, S. E.; Heenan, R. K.; Dyer, R.; Eastoe, J. Low Fluorine Content CO_2-philic Surfactants. *Langmuir* **2011**, *27*, 10562-10569.

(31) Horch, R. A.; Shahid, N.; Mistry, A. S.; Timmer, M. D.; Mikos, A. G.; Barron, A. R. Nanoreinforcement of Poly(propylene fumarate)-based Networks with Surface Modified Alumoxane Nanoparticles for Bone Tissue Engineering. *Biomacromolecules* **2004**, *5*, 1990-1998.

(32) Alexander, S.; Morrow, L.; Lord, A. M.; Dunnill, C. W.; Barron, A. R. pH-Responsive Octylamine Coupling Modification of Carboxylated Aluminium Oxide Surfaces. *J. Mater. Chem. A* **2015**, *3*, 10052-10059.

(33) Bethley, C. E.; Aitken, C. L.; Harlan, C. J.; Koide, Y.; Bott, S. G.; Barron, A. R. Structural Characterization Of Dialkylaluminum Carboxylates: Models for Carboxylate Alumoxanes, *Organometallics* **1997**, *16*, 329-341.

(34) Koide,Y.; Barron, A. R. $[Al_5(^tBu)_5(\mu_3\text{-}O)_2(\mu_3\text{-}OH)_3(\mu\text{-}OH)_2(\mu\text{-}O_2CPh)_2]$: A Model for the Interaction of Carboxylic Acids With Boehmite. *Organometallics*, 1995, **14**, 4026-4029.

(35) Williams, D. H.; Fleming, I.: *Spectroscopic Methods in Organic Chemistry*; McGraw-Hill, New York, **2008**.

(36) Fukumoto, H.; Nakajima, H.; Kojima, T.; Yamamoto, T. Preparation and Chemical Properties of π-Conjugated Polymers Containing Indigo Unit in the Main Chain. *Materials* **2014**, *7*, 2030-2034.

(37) Pitt, A. R.; Morley, S. D.; Burbidge, N. J.; Quickenden, E. L. The Relationship Between Surfactant Structure and Limiting Values of Surface Tension, in Aqueous Gelatin Solution, with Particular Regard to Multilayer Coating. *Colloids Surf., A* **1996**, *114*, 321-335.

(38) Nishino, T.; Meguro, M.; Nakamae, K.; Matsushita, M.; Ueda, Y. The Lowest Surface Free Energy Based on $-CF_3$ Alignment. *Langmuir* **1999**, *15*, 4321-4323.

(39) Sagisaka, M.; Narumi, T.; Niwase, M.; Narita, S.; Ohata, A.; James, C.; Yoshizawa, A.; Taffin de Givenchy, E.; Guittard, F.; Alexander, S.; Eastoe, J. Hyperbranched Hydrocarbon Surfactants Give Fluorocarbon-like Low Surface Energies. *Langmuir* **2014**, *30*, 6057-6063.

(40) Eastoe, J.; Paul, A.; Rankin, A.; Wat, R.; Penfold, J.; Webster, J.R.P. Fluorinated Nonionic Surfactants Bearing Either CF_3- Or H-CF_2- Terminal Groups: Adsorption at the Surface of Aqueous Solutions *Langmuir*, **2001**, 17, 7873-7878.

(41) Downer, A.; Pitt, A.R.; Simister, E.A.; Penfold, J.; Eastoe, J. Effects of Hydrophobic Chain Structure on Adsorption of Fluorocarbon Surfactants with Either CF_3- Or H-CF_2- Terminal Groups. *Langmuir*, **1999**,*15*, 7591-7599.

(42) Wenzel, R. N. Resistance of Solid Surfaces to Wetting By Water. *Ind. Eng. Chem.* **1936**, *28*, 988-994.

(43) Cassie, A. B. D.; Baxter, S. Wettability of Porous Surfaces. *Trans. Faraday Soc.* **1944**, *40*, 546-551.

(44) Erbil, H. Y.; Demirel, A. L.; Avci, Y.; Mert, O. Transformation of a Simple Plastic into a Superhydrophobic. *Science* **2003**, *299*, 1377-1380.

For TOC only

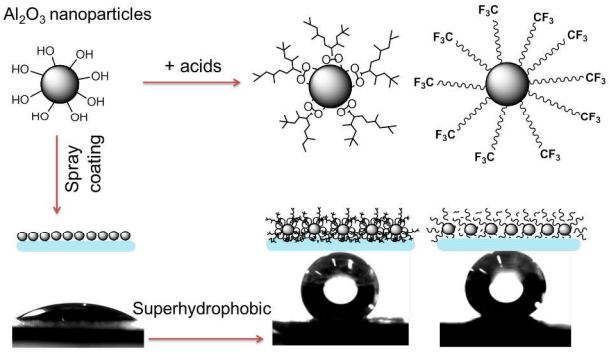
Al_2O_3 nanoparticles
+ acids
Spray coating
Superhydrophobic